

Journal Pre-proof

Unraveling adaptive changes in electric-vehicle charging behavior towards the post-pandemic era by federated meta-learning

Linlin You, Rui Zhu, Mei-Po Kwan, Min Chen, Fan Zhang, Bisheng Yang, Man Sing Wong, Zheng Qin



PII: S2666-6758(24)00025-0

DOI: <https://doi.org/10.1016/j.xinn.2024.100587>

Reference: XINN 100587

To appear in: *The Innovation*

Received Date: 11 August 2023

Revised Date: 5 February 2024

Accepted Date: 5 February 2024

Please cite this article as: You, L., Zhu, R., Kwan, M.-P., Chen, M., Zhang, F., Yang, B., Wong, M.S., Qin, Z., Unraveling adaptive changes in electric-vehicle charging behavior towards the post-pandemic era by federated meta-learning, *The Innovation* (2024), doi: <https://doi.org/10.1016/j.xinn.2024.100587>.

This is a PDF file of an article that has undergone enhancements after acceptance, such as the addition of a cover page and metadata, and formatting for readability, but it is not yet the definitive version of record. This version will undergo additional copyediting, typesetting and review before it is published in its final form, but we are providing this version to give early visibility of the article. Please note that, during the production process, errors may be discovered which could affect the content, and all legal disclaimers that apply to the journal pertain.

© 2024 The Author(s).

Unraveling adaptive changes in electric-vehicle charging behavior towards the post-pandemic era by federated meta-learning

Linlin You,¹ Rui Zhu,^{2,*} Mei-Po Kwan,³ Min Chen,⁴ Fan Zhang,⁵ Bisheng Yang,⁶ Man Sing Wong,⁷ and Zheng Qin²

¹ School of Intelligent Systems Engineering, Sun Yat-Sen University, Shenzhen 518107, China

² Institute of High Performance Computing (IHPC), Agency for Science, Technology and Research (A*STAR), 1 Fusionopolis Way, Singapore 138632, Republic of Singapore

³ Institute of Space and Earth Information Science, the Chinese University of Hong Kong, Hong Kong, China

⁴ Key Laboratory of Virtual Geographic Environment (Ministry of Education), Nanjing Normal University, Nanjing 210023, China

⁵ Institute of Remote Sensing and Geographical Information System, School of Earth and Space Sciences, Peking University, Beijing 100871, China

⁶ State Key Laboratory of Information Engineering in Surveying, Mapping and Remote Sensing, Wuhan University, Wuhan 430079, China

⁷ Department of Land Surveying and Geo-Informatics, The Hong Kong Polytechnic University, Hong Kong, China

* Correspondence email: zhur@ihpc.a-star.edu.sg

Dear Editor,

The electric vehicle (EV) sales have significantly grown over the years to fulfill growing demands for economic travel and greenhouse gas mitigation.¹ However, the surge in the number of EVs has led to charging anxiety as users struggle to find an available charging station before running out of electricity, resulting in longer reserved and waiting time.² Moreover, severe mobility restrictions caused by infectious diseases, such as COVID-19, have greatly affected people's travel behavior^{3,4} and hindered their willingness to use EVs, given that charging in public spaces consumes time and increases the risk of contracting the virus.⁵ This implies that in the post-pandemic era, where individuals coexist with the virus, the interplay between the two important trends, namely vehicle electrification and mobility restrictions, can extensively affect people's daily commuting by using EVs.^{6,7} Hence, it is vital to investigate the interaction between vehicle electrification and mobility restrictions, which is unexplored in the current literature. Since official communications regarding confirmed COVID-19 cases can influence people's travel behavior^{8,9} and EV charging can directly reflect users' propensity to use EVs, quantifying vehicle electrification through EV charging data is an appropriate approach to unravel these interactions. In summary, this study aims to quantify and characterize the interaction between the two trends mentioned above, seeking to understand the diverse influences of confirmed cases and associated factors on EV charging behavior, especially when significant interactions are observed.

We collected all EV charging records, including count (x^c), duration (x^d) in minutes, and volume (x^v) in kWh, from February to May 2022 across 292 Chinese cities. This data encompassed over 240,000 charging piles associated with geo-located 28,000 charging stations. The daily confirmed COVID-19 cases in the local city (i) and neighboring cities are represented as C_i^L and C_i^N , respectively. The study identifies 116 cities for investigation, where the local city has a minimum of 5 confirmed cases, and the daily average charging count exceeds 200 (Figure

1A). Through three correlation analyses (Person, Spearman, and Kendall) and three Granger causality analyses (Likelihood-ratio test, the sum of squares regression-based F test, and chi-square test) conducted on $\{C_i^L, C_i^N\}$ and $\{x^c, x^d, x^v\}$, it was determined that charging behavior in 74 out of the 116 cities was affected by C_i^L and/or C_i^N (Figure 1B). This conclusion is derived from the evidence that $\{C_i^L\}$ and $\{x^c\}$ in each of these cities exhibit the *minimum* correlation coefficient, $\min(|R|)$, greater than 0.1 (Figure 1C) and a *maximum* causative *p*-value smaller than 0.05 (Figure 1D). Furthermore, a similar pattern is also detected for $\{C_i^N\}$ and $\{x^c\}$.

We hypothesized that the changes in charging behavior were influenced by pandemic changes (I^L and I^N), geographical and social conditions (road density e^r and population density e^o), economic conditions (annual per capita disposable income e^i and GDP per capita e^g), and charging capacities (charging pile density e^p and charging station density e^s). Additionally, we considered city-tires, with 14, 17, 29, and 14 cities respectively belong to tiers 1 (the most well-developed cities) to 4. Subsequently, we developed an advanced Federated Meta-learning Model (FMM) comprising Long Short-Term Memory and Multi-Layer Perceptron to estimate the charging behavior on an hourly basis in each city. The 6-fold time-series cross-validation reveals that all the Mean Absolute Errors (MAEs) are less than 10% of the largest observation value for the charging behavior (Figure 1E). Besides, the mean square error, root mean square error, and median square error are remarkably small. These results together indicate that the FMM has attained a highly satisfactory estimation accuracy.

To reveal data distribution patterns, we treated the changes in daily confirmed cases as a positive impulse, equivalent to the standard deviations of $\{C_i^L, C_i^N\}$ over the studied period, denoted by $\{I_i^L, I_i^N\}$. Using the impulse response function, we estimated hourly changes in charging behavior $\{\Delta y_t^c, \Delta y_t^d, \Delta y_t^v\}$ over 24 hours on the selected day when the values hover around the means throughout the entire period. Then, we established a linear impact expression function, $E = [I_*^L, I_*^N, e_*^r, e_*^o, e_*^i, e_*^g, e_*^p, e_*^s]$, to represent independent variables, and the dependent variable, Δy_* , is devoted to express the reaction to the positive impulse. Note that, the subscript “*” represents $\ln(\cdot)$ to better capture non-linear relationships during the analysis. It was found that data distributions between the eight elements of E and Δy_*^c can vary when cities are categorized into different city tiers, levels of GDP per capita, and regions. All elements in E and $\{\Delta y_*^c\}$ approximately follow the Gaussian distribution in each tier, demonstrating unclear linear relationships (Figure 1F).

The aforementioned results motivate us to *quantify* the importance of the eight influential factors in contributing to the changes in charging counts. To achieve this, we calculated the SHapley Additive exPlanations (SHAP) values of the eight factors in E . Specifically, the 50th percentile SHAP values of eight factors are presented in the bottom-right corner of Figures 1G-1R. They are organized into four groups for each category, with $\{\Delta y_*^c\}$ plotted in ascending order on the y-axis. Note that the SHAP values are comparable within the same group since they are obtained from the same model. The results indicate an extremely strong and positive correlation between E and $\{\Delta y_*^c\}$, with the Pearson correlation coefficient R ranging from $[0.86, 0.95]$ ($p \leq 10^{-6}$) for city tiers (Figures 1G-1J), $[0.83, 0.85]$ ($p \leq 10^{-5}$) for GDP per capita levels (Figures 1K-1N), and $[0.88, 0.91]$ ($p \leq 10^{-5}$) for regions (Figures 1O-1R). Additionally, R^2 falls within $[0.75, 0.90]$, $[0.69, 0.73]$, and $[0.70, 0.83]$ for the corresponding three categories, indicating a satisfactory regression for SHAP distribution statistics.

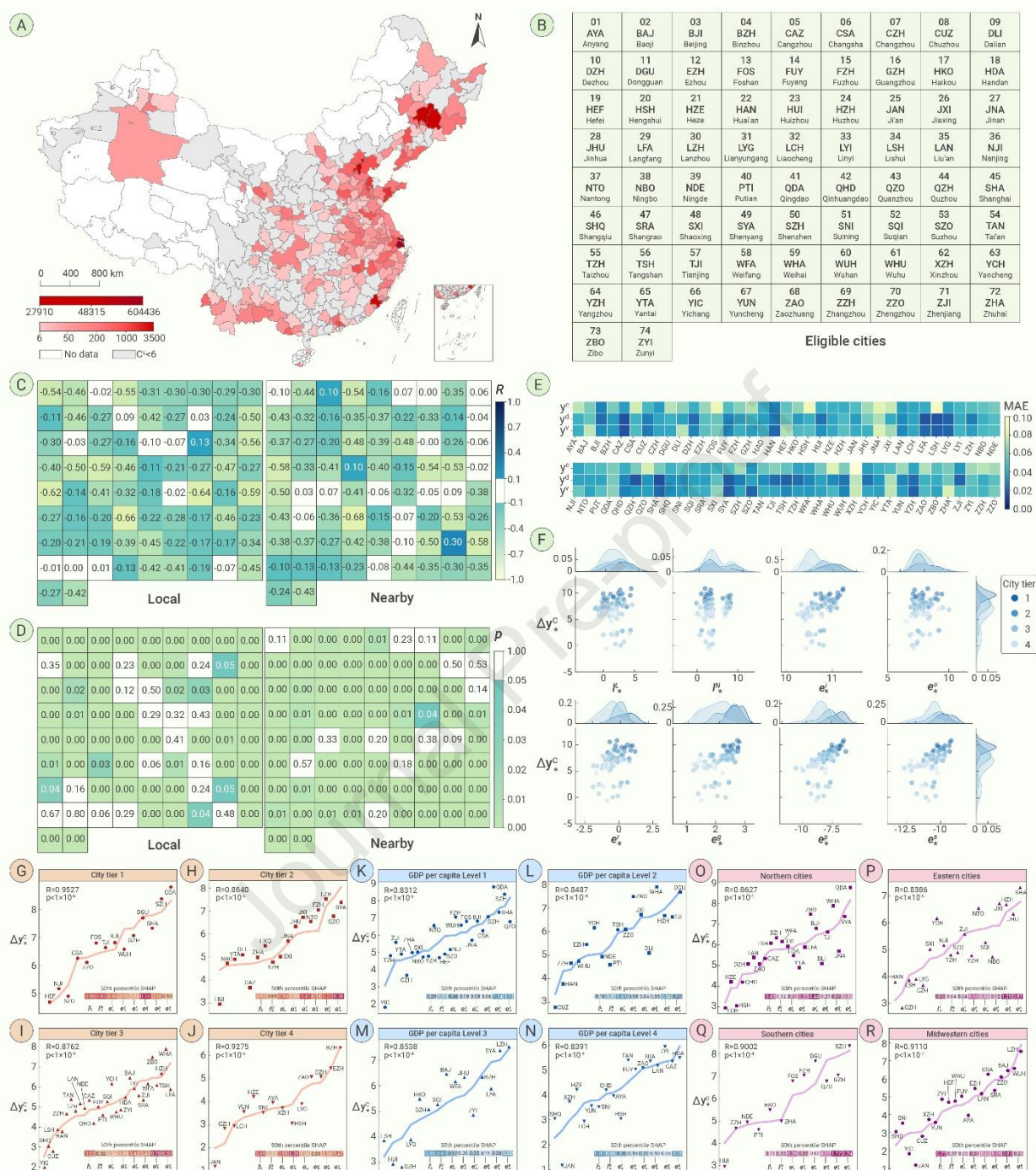


Figure 1. Analysis of hourly EV charging behavior in 74 Chinese cities

(A) The total confirmed cases of cities during the studied period are presented in the red color scheme, and cities with an average daily confirmed cases of fewer than five are marked in gray.

(B) The names and abbreviations of the cities meeting the investigation criteria are listed, corresponding to the grid locations in C and D.

(C) The correlation coefficient of each city, where its absolute value is the minimum among the three correlation coefficients.

(D) The maximum *p*-value of each city among the three types of Granger causality tests.

(E) All the MAEs of the estimated charging count, charging duration, and charging volume in the 74 cities are smaller than 0.01.

(F) The data

distribution between E and $\{\Delta y_*^c\}$ is categorized by the four city-tiers. (G-J) The analysis is categorized into four city-tiers. (K-N) The analysis is categorized by four levels of GDP per capita. Three percentile shreds [50%, 75%, 90%] are used to separate the cities into four levels. (O-R) The analysis is categorized into four regions, defined as the northern, eastern, southern, and midwestern regions.

The results reveal that the 74 affected cities are predominantly situated in the three most dynamic economic zones: Beijing-Tianjin-Hebei, Yangtze River Delta, and Pearl River Delta. This is likely due to the high population density, and it requires relatively high travel demands in these cities to carry out socio-economic activities, potentially resulting in an easier spread of the virus. With 74 out of the 292 cities being affected, it implies that only a few major cities were affected and experienced dynamic changes in charging behavior in response to varying pandemic situations. In comparison to the benchmark without new cases reported in late May 2022, the reduced charging count was less than 25% for 68% of the cities and less than 10% for 79% of the first-tier cities. This suggests that the prevention measures had some impact on EV travel, and the effect was, however, not dramatic. Despite the three megacities in China, i.e., Beijing, Guangzhou, and Shenzhen, experienced a slight decrease in the daily average charging count by 0.55-5.11%, their charging duration or volume, on the contrary, increased by 0.04-5.75%. Moreover, Yangzhou, a second-tier city in Jiangsu province, had a 16.17% reduction in charging count while obtaining a significant increase in charging duration (8.28%) and volume (15.23%). These findings reveal adaptive travel behavior with EVs and a preference for switching to the fast-charging mode to maintain the travel capability while reducing unnecessary exposure.

This study employed the theory of “*the universal visitation law of human mobility*”⁹ to model the accumulated influence of *influential* cases from nearby cities. The influence follows a Gaussian distribution, declining based on the *traveling distance* from nearby cities to the local city, with the maximum distance set at 500 km, encompassing most nearby cities on a large geographical scale in China. Therefore, the model allows us, from a uniquely spatio-temporal perspective, to understand the affected charging behavior. Still taking Yangzhou as an example, it reveals that the city was typically affected by the pandemics occurring in its nearby cities, indicating that the changed charging behavior was to confront the expected upcoming new waves and implying that people’s prevention awareness has increased.

Notably, 81%, 65%, and 70% of the cities respectively obtained a negative Δy^c , Δy^d , and Δy^v response to the positive impulse of $\{I^L, I^N\}$. This indicates that charging duration and volume exhibited a weaker decreasing trend compared to charging count, suggesting that people, overall, adopted adaptive charging behavior by reducing the charging frequency while attempting to maintain charging capability to avoid unnecessary exposure risks when confronting new cases in the local and nearby cities. In detail, the shares of negative (Δy^c , Δy^d , Δy^v) are (71%, 50%, 50%), (94%, 71%, 71%), (90%, 72%, 79%), and (57%, 57%, 71%) for cities in tiers 1 to 4. This reveals two important phenomena. First, cities in tiers 1 to 3 followed the same overall trend, and tier-1 cities experienced the smallest reduction of the three charging behavior, indicating that people in large cities were more likely to keep traveling to carry out socio-economic activities. Second, small cities, on the contrary, were less influenced by new waves, given that only 57% of the tier-4 cities got a decreased charging count, much smaller than cities in tiers 2 and 3.

The 50th percentile of the SHAP values reveals that the impulse of confirmed cases ($\{I_*^L, I_*^L\}$) significantly affected the changes in charging counts (Δy_*^c) in tier-1 cities. However, $\{I_*^L, I_*^L\}$ became less important for cities in tiers 2 to 4. From another perspective, $\{I_*^L, I_*^L\}$ was unimportant for cities where people are generally wealthier (corresponding to GDP per capita levels 1 and 2), while the trend was opposite in levels 3 and 4. This demonstrates that cities with wealthier populations had a better capability in resisting the impulse of the epidemic, implying a similar phenomenon that high-income individuals could prevent infection more effectively during the massive lockdowns.¹⁰

For eastern and southern cities where people are generally well-paid, we observed a similar result that $\{I_*^L, I_*^N\}$ was unimportant, while the charging capacity of e_*^p and e_*^s conclusively affected Δy_*^c . In contrast, both (I_*^L, e_*^r) in northern cities and (I_*^L, e_*^p) in midwestern cities made important contributions to Δy_*^c . This allows us to draw several important suggestions. First, charging behavior in tier-1 cities, with a large economy size and requiring frequent socio-economic activities, could be easily affected by the pandemic. Second, cities with a higher GDP per capita tended to enable citizens to resist the shock of the pandemic better, as I_*^L and I_*^N were basically unimportant. Third, less-developed cities, such as those in tier 4, GDP per capita level 4, and midwestern China, were more sensitive to I_*^L than I_*^N , while well-developed cities presented an opposite trend.

Our findings indicate that adaptive and instantaneous changes exist in charging behavior, responding to pandemic changes and socio-economic conditions. To facilitate the vehicle electrification process, more charging piles or stations can be built at high-demand locations to relieve charging anxiety. Besides, scheduling service related to charging count, duration, volume, and location can be provided to guide convenient travel and increase the usage ratio of charging piles. This encourages professionals in geography, renewable energy, transportation, public health, and policy research to devise new strategies for the post-pandemic era. Furthermore, the proposed analytical method, coupled with the developed FMM, offers a new approach to reveal socio-economic phenomena hidden in complex urban systems.

REFERENCES

1. Heidrich, O., Dissanayake, D., Lambert, S., et al. (2022). How cities can drive the electric vehicle revolution. *Nature Electronics* **5**, 11–13.
2. Bonges III, H.A., and Lusk, A.C. (2016). Addressing electric vehicle (EV) sales and range anxiety through parking layout, policy and regulation. *Transportation Research Part A* **83**, 63–73.
3. Mawani, M., and Li, C. (2020). Coronavirus Disease (COVID-19); Lessons Learnt from International Response and Advice to the Georgia Government. *The Innovation* **1**(2), 100025.
4. Zhu, R., Anselin, L., Batty, M., et al. (2022). The effect of different travel modes and travel destinations on COVID-19 transmission in global cities. *Science Bulletin* **67**, 588-592.
5. Zhou, K., Hu, D., and Li, F. (2022). Impact of COVID-19 on private driving behavior: Evidence from electric vehicle charging data. *Transport Policy* **125**, 164–178.
6. Cai, J., Deng, X., Yang, J., et al. (2022). Modeling transmission of SARS-CoV-2 Omicron in China. *Nature Medicine* **28**, 1468–1475.
7. Colbourn, T. (2020). Unlocking UK COVID-19 policy. *The Lancet Public Health* **5**(7), e362–e363.

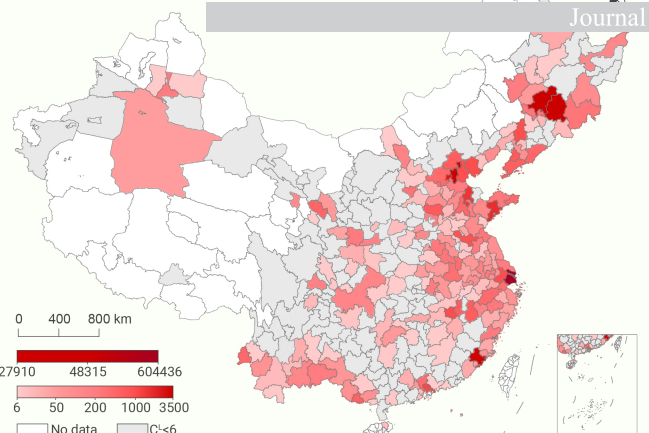
8. Chen, Y., and Lin, B. (2022). Are consumers in China's major cities happy with charging infrastructure for electric vehicles? *Applied Energy* **327**, 120082.
9. Schläpfer, M., Dong, L., O'Keeffe, K., et al. (2021). The universal visitation law of human mobility. *Nature* **593**, 522–527.
10. Jay, J., Bor, J., Nsoesie, E.O., et al. (2020). Neighborhood income and physical distancing during the COVID-19 pandemic in the United States. *Nature Human Behavior* **4**, 1294–1302.

ACKNOWLEDGMENTS

This paper was supported by the National Natural Science Foundation of China (62002398) and the GuangDong Basic and Applied Basic Research Foundation (2023A1515012895), China; and Social Sciences Innovation Seed Fund (ID: C211618002) at A*STAR, Singapore. We also appreciate constructive comments from Prof. Carlo Ratti, Prof. Paolo Santi, Prof. Jinyue Yan, Prof. Chunming Rong, Prof. Biyu Chen, and Dr. Wei Luo.

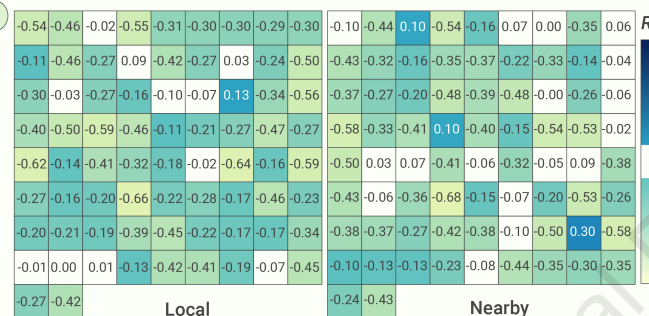
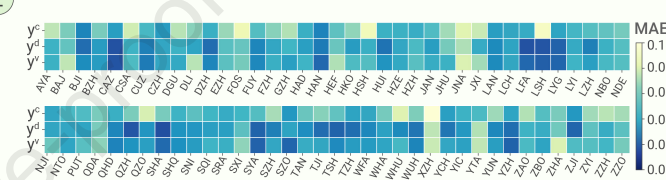
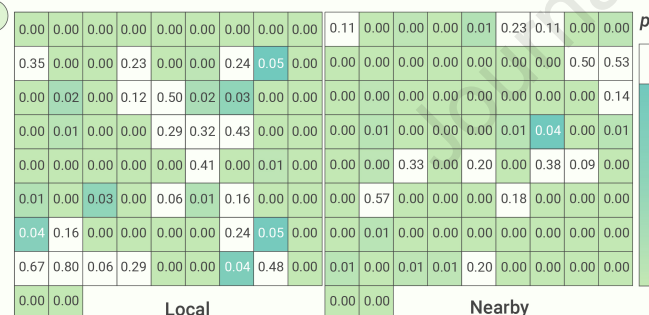
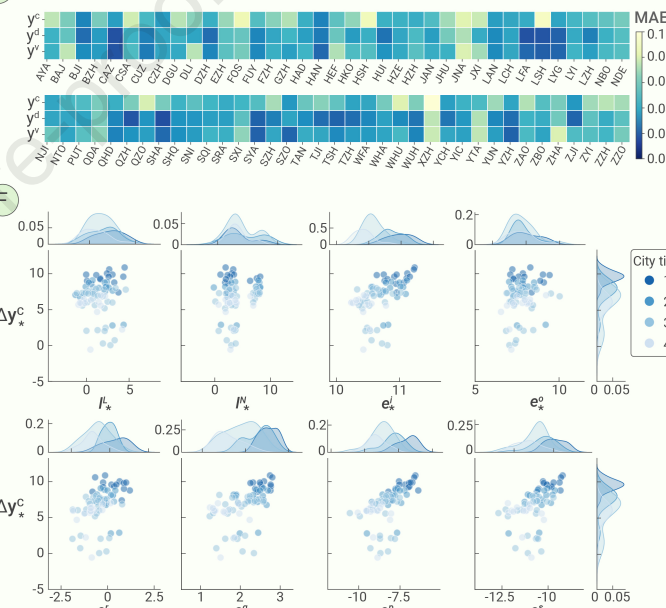
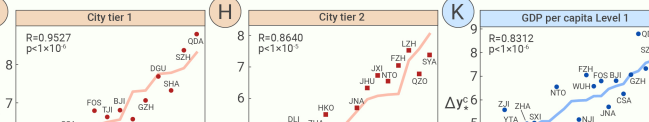
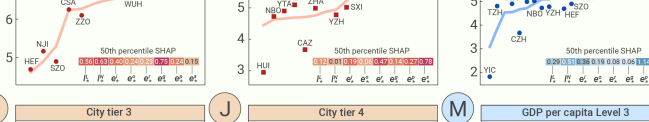
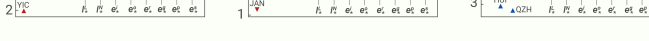
DECLARATION OF INTERESTS

The authors declare no competing interests.

A**B**

01	AYA	02	BAJ	03	BJI	04	BZH	05	CAZ	06	CSA	07	CZH	08	CUZ	09	DLI
DZH	Dezhou	DGU	Dongguan	EZH	Ezhou	FOS	Foshan	FUY	Fuyang	FZH	Fuzhou	16	GZH	Changzhou	17	HKO	
19	HEF	HSH	Hengshui	21	HZE	Haze	22	HAN	Huainan	23	HUI	Huzhou	25	JAN	Jianchang	27	JNA
28	JHU	LFA	Langfang	30	LZH	Lanzhou	31	LCH	Liaocheng	32	LYI	Linyi	33	LSH	Lishui	35	LAN
37	NTO	NBO	Ningbo	39	NDE	Ningde	40	PTI	Putian	41	QDA	Qingdao	42	QHD	Qinhuangdao	43	QZH
46	SHQ	Shangqiu	47	SRA	Shangrao	48	SXI	Shaoxing	49	SYA	Shenyang	50	SZH	Shenzhen	51	SNI	
55	TZH	Taizhou	56	TSH	Tangshan	57	TJI	Tianjin	58	WFA	Weifang	59	WHA	Weihai	60	WUH	
64	YZH	Yangzhou	65	YTA	Yantai	66	YIC	Yichang	67	YUN	Yuncheng	68	ZAO	Zaozhuang	69	ZHH	
73	ZBO	Zibo	74	ZYI	Zunyi	75	ZYI	Zunyi	76	ZZH	Zhangzhou	77	ZJL	Zhenjiang	78	ZHA	

Eligible cities

C**E****D****F****G****H****I****J****K****L****M****N****O****P****Q****R**